

SELF-ALIGNED MICRO CONTACT PRINTING USING MEMS

K. Choonee¹, R.R.A. Syms^{1}, and H. Zou²*

¹EEE Dept., Imperial College London, Exhibition Road, London SW7 2AZ, UK

²School of Mechanical Engineering, Dalian University of Technology, Dalian 116024, P R CHINA

ABSTRACT

Aligned, multilevel micro contact printing without dedicated printing equipment is demonstrated. Miniature print engines are constructed from silicon parts using MEMS technology. The method is extended to include electrostatically driven patterning of flexible substrates.

KEYWORDS

Micro contact printing, electrostatic, MEMS

INTRODUCTION

Micro Contact Printing (μ CP)

Micro contact printing (μ CP) is a highly flexible method of surface patterning at the nanoscale [1]. The method is based on moulded stamps formed in the soft elastomer polydimethylsiloxane (PDMS), used in conjunction with an ink that can form a self-assembled monolayer on a suitably coated surface as shown in Figure 1 [2]. Suitable combinations of ink and substrate include alkanethiols such as hexadecanethiol on metals such as Au. The SAM can act as a resist against weak chemical etchants, allowing the pattern to be transferred to the surface coating with an overall resolution of around 100 nm [3]. Other processes may be used to transfer the pattern into the substrate. The surface properties of the SAM may be modified to control protein adsorption, allowing widespread applications in biochemistry and biology.

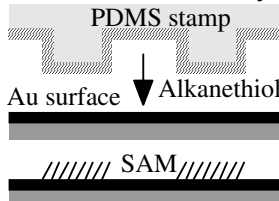


Figure 1. Micro contact printing.

Self Aligned μ CP using MEMS

We have recently developed a self contained MEMS based printing engine which includes the print head, the suspension, an alignment system and an actuation mechanism [4]. The latter contains a movable block carrying a soft stamp and supported on an elastic suspension allowing out-of-plane deflection. The engine's surround is grooved so that it may mate with a rail pattern. The device can be constructed from silicon-compatible materials using standard micro-fabrication. Parts requiring mechanical strength (the print head and the surround) are formed in the substrate, while flexible parts (the suspension) are formed in a thinner surface layer. The

stamp is formed by spray coating PDMS on the structured print head.

Prototype devices have been fabricated in a (100) mm diameter, wafer-scale batch in both single crystal and bonded silicon on insulator material, using a STS ICP DRIE tool. Figure 2 shows a completed device in single crystal Si, which contains a 5 mm x 5 mm print head supported on a torsional suspension system within a 10 mm x 10 mm frame, which also contains the alignment groove. The print head carries a $\sim 10\mu\text{m}$ high bar pattern defined by optical lithography with micron-scale resolution.

Target substrates containing compatible self-alignment features were constructed by fabricating pairs of proud parallel rails in single crystal silicon by KOH etching. The Si surface was then sputter coated with Au to allow alkanethiol SAM formation. The print engines self-align to the rail pattern approximately 30 μm above the substrate as shown in Figure 3.

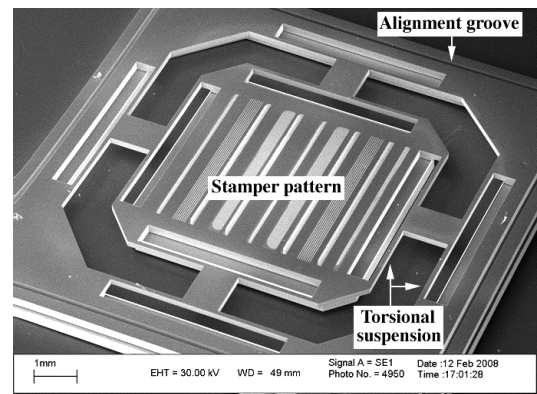


Figure 2. SEM of silicon micro contact printing engine

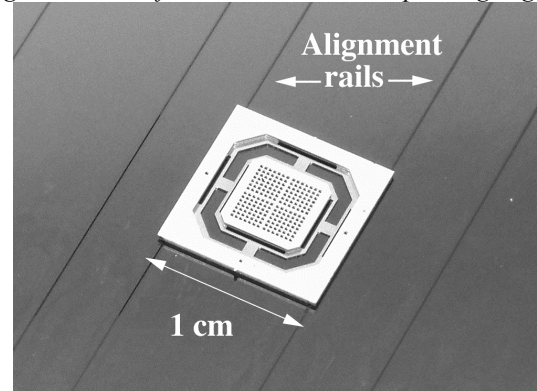


Figure 3. Printing engine mounted on alignment rails.

The individual engines were then spray-coated with PDMS to form a stamp layer capable of alkanethiol adsorption and conformal contact. Mixtures of Dow

Corning PDMS were used to create a solution with a low viscosity for spray coating. Sylgard 184 was mixed with 184 curing agent and 200 Fluid 20 cs (which has a much lower viscosity) in the proportions 1: 0.1: 1 and applied through a stencil using a modeller's airbrush driven with pressurised N₂. The PDMS was then cured at 100°C for 15 mins, and its surface was washed in ethanol to extract any uncured siloxane. Figure 4 shows a stamp formed by this method.

The alignment grooves on the engine interlock with alignment features on the target substrate, and hence the process is self-aligning and parallelism may be set without contact as shown in Figure 5. The device can be driven either manually or electrostatically, by applying a voltage between the engine and the substrate. The former has yielded excellent results as shown in Figure 6, but the latter has been more problematic due to electrostatic discharge caused by the high operating voltages inherent at a large (30 μm) separation.

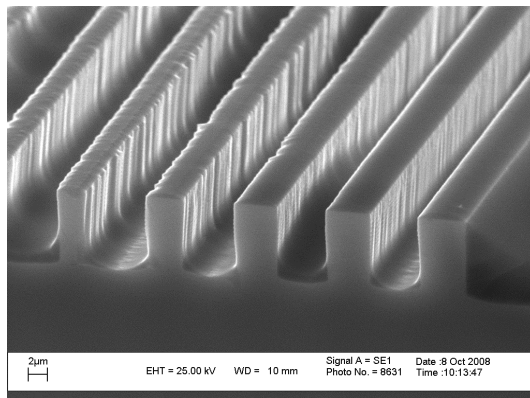


Figure 4. PDMS spray coated structures.

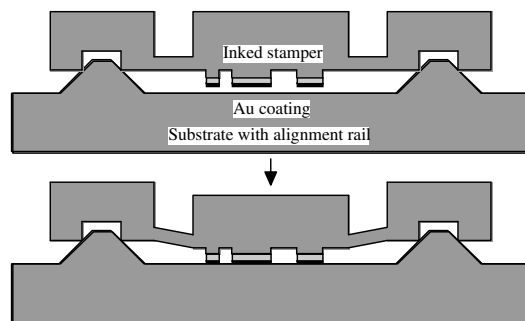


Figure 5. Operation of μCP engine. Actuation can currently be either manual or electrostatic.

Micro contact printing was carried out using 1-hexadecanethiol, which was diluted 1 mMol in ethanol. Stamps were coated in ink using a brush and then dried in N₂. Manual pattern transfer was achieved by contacting the stamp to Si surfaces coated with 30 nm Au. Exposed Au was then etched using a solution of potassium thiosulphate (K₂S₂O₃, 0.1 M), potassium hydroxide (KOH, 1 M) and potassium ferricyanide (K₃Fe(CN)₆, 0.01 M), a weak etchant that can achieve a high etch rate (5 nm/min)

without significant damage to alkanethiol SAMs. Multilayer printing can be achieved by inking the stamp, printing, cleaning, re-inking, rotating the stamp by 90 degrees and printing a second time. Figure 6 shows a multilayer pattern after printing and Au etching. Here the orthogonal sets of bars correspond to consecutive imprints.

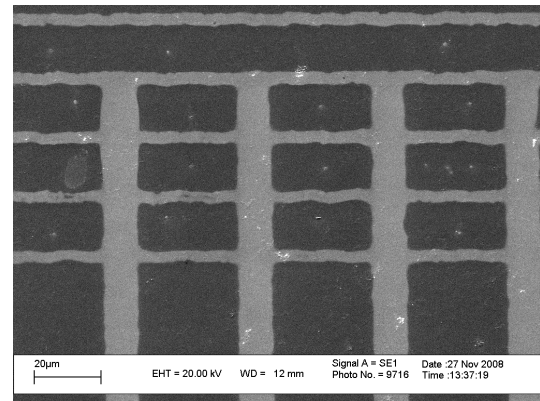


Figure 6. Result of aligned multilayer printing.

ELECTROSTATIC μCP

Our previous work [4] has shown that electrostatic μCP using MEMS is possible, but suffers from discharge due to high pull-in voltages and poor insulation. Here we present a new electrostatic printing mode where a thick insulating PDMS stamp is kept stationary and a thin flexible gold coated polyimide membrane, which acts as substrate, is deflected to make contact. The reduction in stiffness of the movable part greatly reduces actuation voltages, minimising discharge effects.

Improved PDMS Stamps

A new method of depositing the PDMS layer is demonstrated. First a uniform layer (~10s of μm thick) of PDMS is sprayed onto the target surface. The layer is then embossed against a structured Si master and then thermally cured. An anti-stiction coating, such as the passivation layer of the STS ICP DRIE, is required to enable separation. Figure 7 shows this process as applied to the MEMS printing engine. Figure 8 shows part of the cross section of the 30 μm thick stamp formed with this method and used to perform electrostatic μCP.

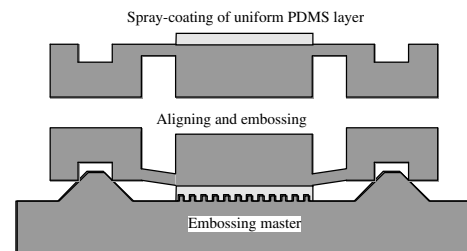


Figure 7. Spraying and embossing of PDMS stamp.

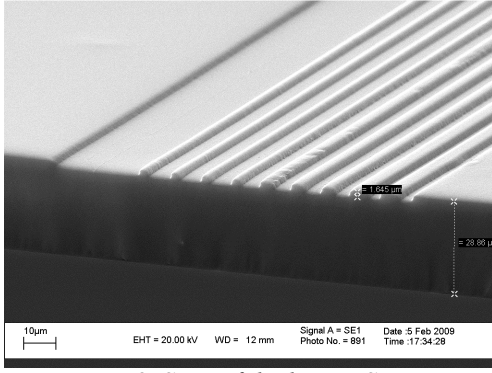


Figure 8. SEM of thick PDMS stamp

Experimental Setup

Figure 9 shows the arrangement for membrane-based electrostatic μ CP. The stamp is $\sim 30 \mu\text{m}$ thick slab of PDMS formed on a doped piece of n-Si wafer as described above. The patterned stamp area measures $\sim 5 \text{ mm} \times 3 \text{ mm}$ and consists of recessed parallel lines with widths ranging from $5 \mu\text{m}$ to $20 \mu\text{m}$. A further gold layer is included at the base of the structure for electrical contact. The flying height of the membrane is set by the thickness of the spacer, which is a $25 \mu\text{m}$ polyimide film sputter coated with $\sim 80 \text{ nm}$ of Au for electrical contact. The membrane itself is $\sim 12 \mu\text{m}$ thick polyimide with a $\sim 30 \text{ nm}$ Au layer on the bottom side, and a $\sim 80 \text{ nm}$ Au layer on the top (not shown). The upper layer Au coating was included to increase the reflectivity of the surface during interferometric measurement. The membrane is effectively 6 mm long and 3 mm wide, and is simply supported on three sides and free on the fourth.

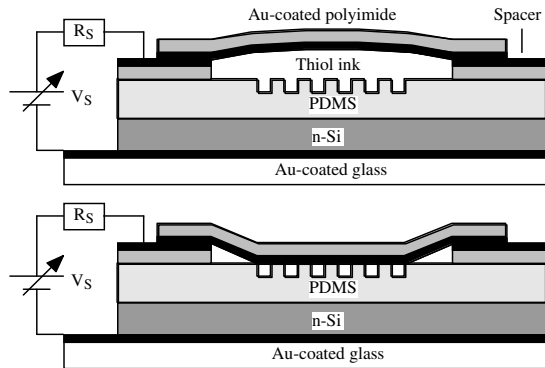


Figure 9. Membrane-based electrostatic μ CP.

Membrane Deflection Profile

The behaviour of a rectangular membrane is governed by the differential equation [5]:

$$\partial^4 w / \partial x^4 + 2\partial^2 w / \partial x^2 \partial y^2 + \partial^4 w / \partial y^4 = q/D \quad (1)$$

Here w represents the deflection at a point (x, y) in the plane of the plate, q is the pressure distribution, and D is the flexural rigidity. Approximate solutions for different boundary conditions have been tabulated [6] but these are usually valid for small deflections (relative to the plate

thickness). In our case, a $12 \mu\text{m}$ film is displaced by $\sim 25 \mu\text{m}$ and the strains in the middle plane of the plate due to bending are appreciable. This so called diaphragm stress cannot be neglected [5, 6]. Furthermore, the membrane is Au-coated, and this induces further stress and pre-distortion in the film. These constraints make the arrangement hard to model and beyond the scope of this paper. Experimental results are therefore presented instead.

The deflection profile of the membrane was monitored using a scanning white light interferometer (Wyko NT9100, Veeco Inc.). As the applied voltage was increased, the membrane was observed to bend slightly about the edge of the spacer before suddenly buckling and contacting the PDMS stamp as shown in Figure 10. After initial contact was made, the total contact area was observed to increase with increasing voltage. Cross sections of the membrane at different applied voltages are shown in Figure 11. At a voltage of $\sim 700 \text{ V}$, practically all the patterned stamp area is contacted.

Note that the gaps in the data correspond to the inclined regions of the membrane. For these regions, the reflected light is not captured in the imaging lens of the interferometer due to its limited numerical aperture.

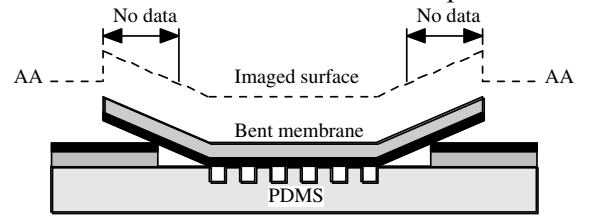


Figure 10. Membrane cross-section during imaging. The inclined segments are not reliably captured. Surfaces AA represent the flat spacer surface which is the reference plane

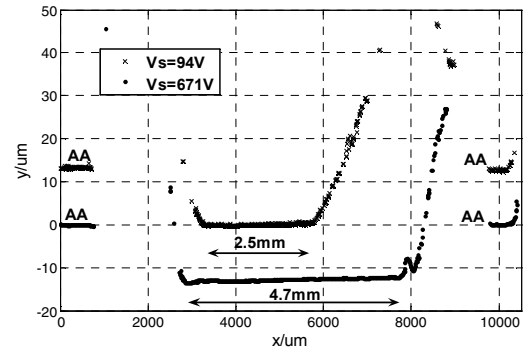


Figure 11. Deflection of membrane at different voltages μ CP Results

Figure 12a shows an electrostatically printed pattern, printed at an applied voltage of $\sim 700 \text{ V}$, following inking and wet chemical etching as described in the previous section. The Au pattern has varying linewidths ranging from $\sim 2 \mu\text{m}$ to $\sim 30 \mu\text{m}$. Figure 12b highlights the pattern fidelity for $10 \mu\text{m}$ wide lines spaced by $25 \mu\text{m}$.

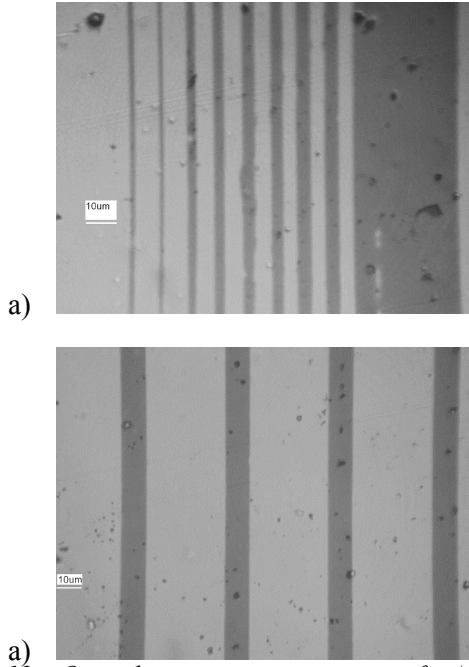


Figure 12. Optical microscope images of a) varying linewidths. and (b) 10µm wide lines. The darker regions are polyimide and the bright regions are Au.

Discussion

The geometry of Figure 9 can be modeled approximately as a parallel plate capacitor with two dielectric layers as shown in Figure 13, which can be analyzed as a series arrangement capacitors of the same cross-sectional area. It can be shown that for an applied voltage V_S , the voltages distributed across the two capacitors are as follows:

$$V_{PDMS}/V_S = 1/(1 + \epsilon_r S_{air}/S_{PDMS}) \quad (2)$$

$$V_{air}/V_S = \epsilon_r/(\epsilon_r + S_{PDMS}/S_{air}) \quad (3)$$

Therefore, as the membrane deflects downwards, S_{air} tends to zero, so V_p/V_S tends to unity, while V_{air}/V_S tends to zero. Thus, during the snap-down phase of electrostatic printing, most of the voltage is dropped across the PDMS stamp rather than the air gap, thereby avoiding electrostatic discharge despite the high actuation voltage. This form of stabilizing capacitive feedback was initially proposed in [7] as a means of extending the travel range of electrostatic actuators.

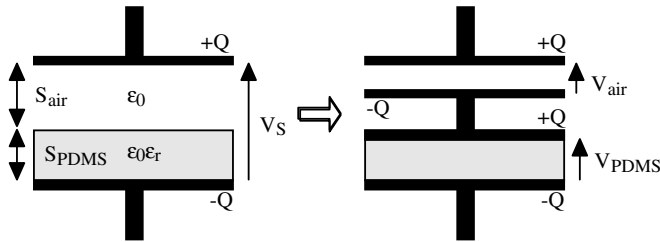


Figure 13. Electrical model of membrane and stamp

CONCLUSION

We have demonstrated multilevel self-aligned patterning of Au using prototype silicon μ CP engines. We have also shown that electrostatically driven μ CP can be carried out on flexible membranes with a suitable stamp. Work is continuing to extend electrostatic μ CP to large area membranes with self-alignment capability. Important issues will include quantifying and minimizing the pattern distortion and the alignment mismatch caused by any stretching of the membrane during contact.

ACKNOWLEDGEMENTS

The authors are grateful to Dr Man Niang Kham for help with interferometric imaging.

REFERENCES

- [1] Kumar A., and Whitesides G.M. "Features of gold having micrometer to centimeter dimensions can be formed through a combination of stamping with an elastomeric stamp and an alkanethiol "ink" followed by chemical etching" *Applied Physics Letters*, vol. 63, no. 14, pp. 2002-2004, 1993.
- [2] Bain C.D., Troughton E.B., Tao Y.T., Evall J., Whitesides G.M., and Nuzzo R.G. "Formation of monolayer films by the spontaneous assembly of organic thiols from solution onto gold" *Journal of the American Chemical Society*, vol. 111, no. 1, pp. 321-335, 1989.
- [3] Xia Y., and Whitesides G.M. "Soft Lithography" *Angewandte Chemie International Edition*, vol. 37, no. 5, pp. 550-575, 1998.
- [4] Syms R.R.A., Zou H., Choonee K., and Lawes, R.A. "Silicon microcontact printing engines" *Journal of Micromechanics and Microengineering*, vol. 19, no. 2, pp. 025027, 2009.
- [5] Timoshenko S.P. and Woinowsky-Krieger S. "Theory of Plates and Shells" 2nd ed.: McGraw Hill Book Co., 1959.
- [6] Young W.C. "Roark's formulas for stress and strain" 6th ed., New York: McGraw Hill Book Co., 1989.
- [7] Seeger J.I., and Crary S.B. "Stabilization of electrostatically actuated mechanical devices" *Int. Conf. on Solid State Sensors and Actuators, TRANSDUCERS '97 Chicago.*, vol. 2, pp. 1133-1136, 1997.

CONTACT

* R.R.A. Syms, tel: +44(0)207-594-6203; email: r.syms@ic.ac.uk